metals

MDPI

Article

Robust Ag-Cu Sintering Bonding at 160 °C via Combining Ag_2O Microparticle Paste and Pt-Catalyzed Formic Acid Vapor

Liangliang He [1,2,3,†], Junlong Li [1,2,3,†], Xin Wu [4], Fengwen Mu [5,6,*], Yinghui Wang [1,2,3,*], Yangting Lu [3] and Tadatomo Suga [3,5]

1 Institute of Microelectronics of Chinese Academy of Sciences, Beijing 100029, China; heliangliang@ime.ac.cn (L.H.); lijunlong@ime.ac.cn (J.L.)
2 University of Chinese Academy of Sciences, Beijing 100049, China
3 Kunshan Branch, Institute of Microelectronics of Chinese Academy of Sciences, Suzhou 100049, China; luyangting@ksime.com (Y.L.); suga@pe.t.u-tokyo.ac.jp (T.S.)
4 Department of Mechanical and Materials Engineering, College of Engineering and Applied Science, University of Cincinnati, Cincinnati, OH 45221, USA; xinwu350@gmail.com
5 Collaborative Research Center, Meisei University, Hino-shi, Tokyo 1918506, Japan
6 Kagami Memorial Research Institute for Materials Science and Technology, Waseda University, Shinjuku, Tokyo 1690051, Japan
* Correspondence: mufengwen123@gmail.com (F.M.); wangyinghui@ime.ac.cn (Y.W.); Tel.: +81-04-2591-5219 (F.M.); +86-512-5031-6765 (Y.W.)
† These authors contribute equally to this work.

Received: 9 February 2020; Accepted: 26 February 2020; Published: 28 February 2020

Abstract: With the assistance of Pt-catalyzed formic acid vapor, robust Ag-Cu bonding was realized at an ultra-low temperature of 160 °C under 3 MPa for 30 min via the sintering of Ag nanoparticles in situ generated from Ag_2O microparticles. The Cu oxide layer at the interface after bonding can be eliminated, which improves the bond strength and electrical conductivity of the joint. A metallic bond contact between the sintered Ag and the Cu substrate is obtained without interfacial solid solution and intermetallic phases, and the shear strength is comparable to previous bonding at a higher temperature. The bonding mechanisms were figured out by comparing the bonding with and without the Pt-catalyzed formic acid vapor. This ultra-low temperature Ag-Cu bonding method may create more flexibilities in the structure design and material selection for power device integration.

Keywords: sintering bonding; nanoparticles; Ag_2O microparticle; interface; die attach

1. Introduction

Wide bandgap semiconductors such as SiC and GaN are becoming very promising for the high-power and high-temperature devices, which meanwhile brings new requirements on the die attach materials such as high service temperature, high thermal conductivity, and high reliability [1–5]. Owing to the excellent thermal conductivity and electrical conductivity of Ag, Ag nanoparticles have been widely investigated as a new die attach material for high-power devices [6–11]. However, the wide applications of Ag nanoparticles are largely limited by their high cost [12,13]. Owing to the relative low cost, Cu nanoparticles have been considered as an alternate [14–16]. Nonetheless, Cu is very easily to be oxidized, leading to the difficulties for storage and sintering [17,18]. Besides, the cost of Cu nanoparticles is not yet as low as expected.

Another candidate is Ag_2O microparticles, which are cheaper than Ag nanoparticles. The reduction of Ag_2O microparticles by reducing solvents can produce lots of Ag nanoparticles, which can be

employed for the sintering bonding at a low temperature [13,19,20]. Ag_2O microparticles have already been applied for the bonding of Ag and Au. The joint for Ag-Ag and Au-Au bonding by using Ag_2O microparticles has been demonstrated to be very robust with a shear strength higher than 20 MPa at approximately 250 °C under 2–2.5 MPa [19,20]. Besides, an epitaxial growth of each Ag nanoparticle, aligning the orientation of the original surface, has been confirmed.

In power electronics packaging, Cu is one of the most commonly used materials for electrodes, substrates, and lead frames [21]. Although the metallization of Cu by using Ag or Au can improve the bondability, the bare Cu bonding is meaningful to reduce the cost and simplify the process. In fact, the bonding of bare Cu using Ag micro/nanoparticles in air is also challenged by the problem of interfacial oxidation, which weakens the bond strength and degrades the electrical characteristic of the joint [22]. Some strategies have been proposed that use an inert or reductive gas atmosphere [23,24] or coat the Cu surface by a single layer of graphene [25] to prevent the Cu surface from oxidation during the sintering bonding. Compared to the Cu bonding by Ag micro/nanoparticles, the oxidation problem in the bonding by Ag_2O microparticles is more serious, because oxygen can also come from the decomposition of Ag_2O. To no one's surprise, the Cu bonding using Ag_2O microparticles in previous researches always has a very low bond strength [26]. An interfacial Cu oxide layer is usually observed [26–28]. Takata et al. [26] demonstrated that polyethylene glycol (PEG) when used as the reducing solvent can suppress the interfacial oxidation during sintering bonding using Ag_2O microparticles, owing to the residual of PEG at the sintering temperature. However, a higher bonding temperature (≥300 °C), compared to other reducing solvents such as diethylene glycol (DEG) or triethylene glycol (TEG), is required. A strong Cu bonding via the sintering of Ag_2O microparticles without an interfacial oxide layer has not yet been developed at a low temperature (<300 °C). Since oxygen can also be generated by the decomposition of Ag_2O, an effective reductive gas atmosphere is assumed to be necessary. Recently, we have demonstrated that a Pt-catalyzed formic acid vapor is more effective for the reduction of Cu oxides compared to the normal formic acid vapor, thanks to the generation of H radicals during catalyzation [29–36]. Its combination with Cu nanoparticles sintering can realize a low-temperature Cu bonding with a large surface-oxidation tolerance [16,36].

In this work, we report a strong Ag-Cu bonding via the sintering of the Ag nanoparticles in situ derived from Ag_2O microparticles at an ultra-low temperature of 160 °C. This new ultra-low temperature Ag-Cu bonding method sheds light on new opportunities in the structural design and material selection for power device integration.

2. Experimental

Oxygen-free Cu cylinders with a diameter of 10 mm and a height of 4 mm are used as the Cu specimens for bonding. SiC chips with a size of 6 mm × 6 mm × 0.35 mm cut from a 4-inch SiC wafer were prepared as the dummy device. The bonding side of SiC chips was deposited with 100 nm Ti and 700 nm Ag by sputtering. Ag-Cu bonding was studied in this work, since Ag is widely used as the electrodes for current devices. Before bonding, both the Cu surface and Ag surface were cleaned in acetone, ethanol, and citric acid in an ultrasonic cleaner.

Commercial Ag_2O microparticles (Shanghai Puwei Applied Materials Technology Co., Ltd., Shanghai, China) with a nominal size of approximately 1 µm, as shown in Figure 1, were mixed with ethylene glycol (EG) to form a paste that is suitable for coating, which consists of 40 wt. % EG and 60 wt. % Ag_2O. Thermogravimetric–differential thermal analysis (TG-DTA) was employed to investigate the thermal characteristic of the Ag_2O paste in a flowing N_2 gas at a heating rate of 10 °C/min. The TG-DTA of the Ag_2O microparticles was also analyzed for comparison. To further support the TG-DTA analysis, the microstructure change and decomposition transformation of the Ag_2O paste after heating at 150 °C for 3 min were verified by scanning electron microscopy (SEM, JEOL JSM-7800F, JEOL Ltd., Tokyo, Japan) and X-ray diffraction (XRD, Bruker D8-ADVANCE, Bruker Corporation, Baltimore, MD, USA), respectively.

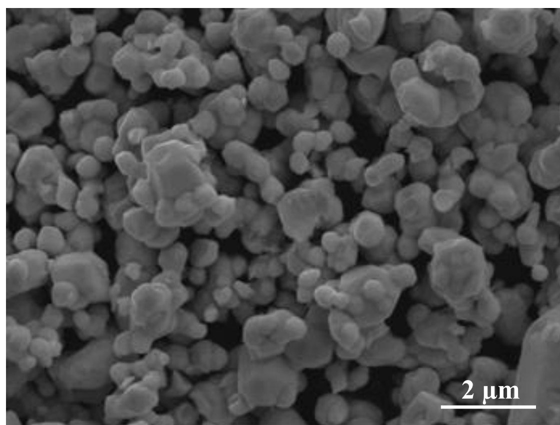

Figure 1. SEM image of Ag_2O microparticles.

The prepared Ag_2O paste was coated on the copper substrate, followed by mounting the SiC chip. The assembled sample is firstly preheated at 150 °C for 5 min and then bonded at 160 °C for 10 min, 20 min, and 30 min with a heating rate of 1 °C/s in a flowing N_2 gas with or without the Pt-catalyzed formic acid vapor, respectively. Prior to the preheating, a pressure of 3 MPa is applied, followed by the feed of Pt-catalyzed formic acid vapor. The H radicals in the Pt-catalyzed formic acid vapor and the remaining formic acid vapor after catalyzation are expected to avoid or reduce the Cu oxides at the interface. The bond strength was measured by a shear strength tester (TRY Precision MFM 1200, Rui Yin (HK) Co., Limited, Hongkong, China) at a speed of 50 µm/s. For every condition, 3–5 samples were tested. The fracture surfaces after shear test were characterized by SEM and energy-dispersive X-ray spectroscopy (EDS) to investigate the fracture behavior. To inspect the microstructure of the sintered layer by SEM, the bonded samples were firstly mechanically cut and then polished by an ion beam. To further investigate the bond interface between sintered Ag and Cu substrate, a focused ion beam (FIB, NVision 40, Zeiss, Oberkochen, Germany) was employed to slice the bonding interface, which was then observed using a scanning transmission electron microscope (STEM, JEOL 2010, JEOL Ltd., Tokyo, Japan) equipped with an EDS. For all of the cross-sectional interface observations, the central part of the bonded sample was employed. In order to further confirm the effect of the Pt-catalyzed formic acid vapor, two Cu specimens coated with Ag_2O paste were heated at 160 °C for 30 min in a flowing N_2 gas with or without the formic acid vapor, respectively. After removal of the sintered layer, X-ray photoelectron spectroscopy (XPS, Thermo escalab 250XI, Thermo Fisher Scientific Inc., Waltham, MA, USA) equipped with a monochromatic Al X-ray radiation source (1486.6 eV) was used to inspect the surface chemical differences between the two Cu specimens. The adsorbed adventitious carbon (C 1s, 284.8 eV) was used as a reference for the calibration of binding energy.

3. Results and Discussion

The TG-DTA results of the Ag_2O paste and Ag_2O microparticles were compared in Figure 2. As shown in Figure 2a, a violently exothermic reaction between EG and Ag_2O microparticles can happen at a temperature as low as approximately 150 °C. As a comparison, the decomposition of Ag_2O microparticles is very slow at a low temperature unless the temperature is higher than 350 °C. According to the weight loss presented in the TG curve, we can assume that all of the Ag_2O has transformed into Ag together with the removal of EG at approximately 150 °C. Figure 3 shows the XRD results of the Ag_2O paste sintered at 150 °C for 3 min in a flowing N_2 gas with or without the formic acid vapor. It can be seen that both of the sintered Ag_2O pastes have become Ag without the residuals of Ag_2O. The microstructures of two kinds of sintered Ag_2O paste were further investigated by SEM, which is shown in Figure 4. Both of them have a typical structure of sintered Ag nanoparticles, which indicates the in situ generation of Ag nanoparticles from Ag_2O reduction. It seems the structure sintered without the formic acid has more clear sintered Ag necks compared to that sintered with

formic acid. One reasonable reason is that the Pt-catalyzed formic acid vapor is helpful for the Ag sintering via reducing the oxygen concentration by its strong reductivity [29–35].

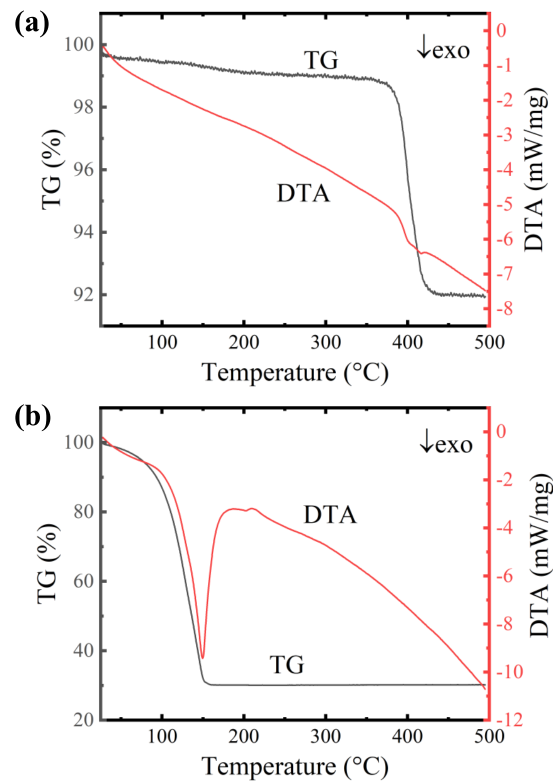

Figure 2. Thermogravimetric–differential thermal analysis (TG/DTA) analysis results of (**a**) the Ag_2O powder and (**b**) the Ag_2O paste with a heating rate of 10 °C/min in flowing N_2 gas.

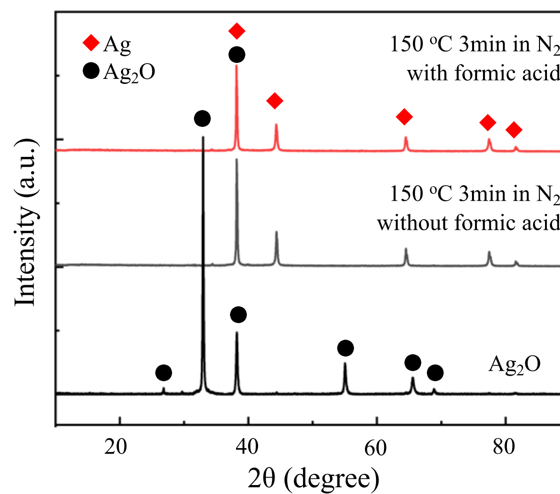

Figure 3. XRD patterns of the Ag_2O paste sintered at 150 °C for 3 min in a flowing N_2 gas with or without the Pt-catalyzed formic acid vapor. Ag_2O was used as a reference.

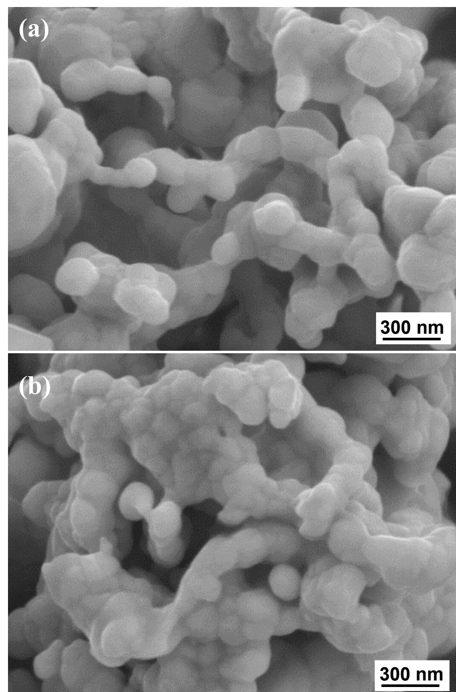

Figure 4. SEM images of the Ag_2O paste sintered at 150 °C for 3 min in a flowing N_2 gas (**a**) with and (**b**) without the Pt-catalyzed formic acid vapor.

In accordance of the thermal characteristic of Ag_2O paste, the bonding was determined to be carried out at 160 °C. The shear strengths of the bonding with or without formic acid vapor are compared in Figure 5. Several previous researches of Ag-Cu or Cu-Cu bonding via Ag_2O microparticles, Ag nanoparticles, or Ag hybrid particles (nano, submicro, and micro) in different atmospheres (air, N_2, and 4% H_2/N_2) at a temperature higher than 250 °C are referred for comparison [23,24,26]. The bonding with the formic acid vapor for 10 min can have an average shear strength as high as approximately 22.8 MPa, which is much higher than that of without the formic acid vapor (approximately 1.1 MPa) and comparable to other bonding via Ag particles at high temperature [23,24]. The increase of bonding time to 20 min brings a slight improvement of shear strength, and there is almost no changes when the bonding time increases to 30 min (approximately 25.7 MPa). For the bonding without the formic acid vapor, the prolonging of the bonding time can remarkably increase the bond strength, but the bonding is still much weaker than that with the formic acid vapor. The further following analyses will focus on the bonding for 30 min, since the bonding without the formic acid vapor can also produce a relatively strong joint.

The fracture surfaces of the Cu substrate side from the samples bonded at 160 °C for 30 min were characterized by SEM to understand the fracture behavior, as shown in Figure 6. Figure 6a,b shows the fractures that happened in the sintered Ag layer. The fracture of the sample with the formic acid vapor, as shown in Figure 6a, has clear ductile fracture traces. As a comparison, the fracture of the sample bonded without the formic acid vapor, as shown in Figure 6b, has far fewer ductile fracture traces, which agrees well with the shear strength result. Figure 6c,d shows that the typical fractures happened at the interface between the sintered Ag layer and the Cu substrate. The corresponding EDS mappings are shown in Figure 6e,f. Obvious differences can be found between the samples bonded with and without the formic acid vapor. For the sample bonded with the formic acid vapor, both unsintered Ag nanoparticles and the sintered Ag with a ductile fracture can be observed on the Cu surface, as shown in Figure 6c. The sintered Ag with a ductile fracture reveals that there is a strong bonding between the sintered Ag and the Cu substrate. On the contrary, for the sample bonded without the formic acid vapor, a number of unsintered fine Ag nanoparticles can be found in Figure 6d. Besides, the Cu surface without the formic acid vapor become much rougher than that with the formic acid vapor, which is

probably caused by a serious oxidation of the Cu surface [37]. This indicates that the Cu surface oxides can be reduced by the formic acid vapor during the sintering bonding, which should contribute to improving the bond strength of the interface between the sintered Ag and the Cu substrate.

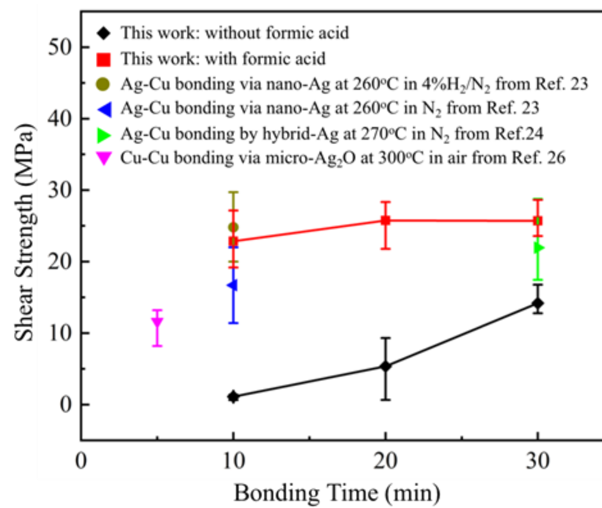

Figure 5. Shear strength of the Ag-Cu bonding at 160 °C under 3 MPa for 10 min, 20 min, and 30 min with and without the formic acid vapor. The referred strength results of the joints bonded at temperatures higher than 250 °C are from the literature [23,24,26].

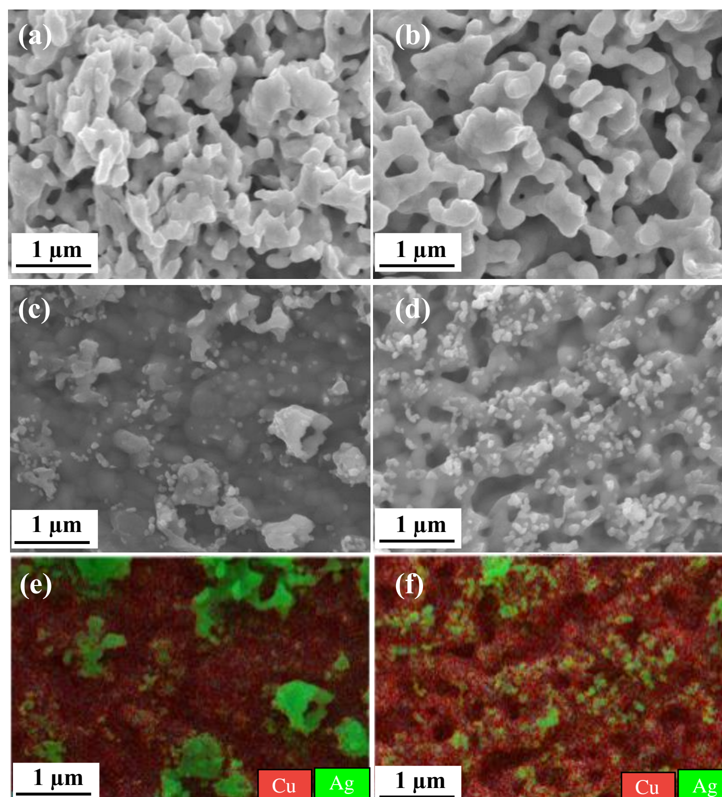

Figure 6. Fracture surfaces of the Cu substrate side from the samples bonded at 160 °C for 30 min. (**a**,**c**): sample bonded with the formic acid vapor; (**b**,**d**): sample bonded without the formic acid vapor; (**a**,**b**): fractures occurred in the sintered Ag layer; (**c**,**d**): fractures occurred at the interface between the sintered Ag layer and the Cu substrate; (**e**,**f**) are the energy-dispersive X-ray spectroscopy (EDS) mapping corresponding to (**c**,**d**), respectively. Red and green represent Cu and Ag, respectively.

The interfacial microstructures of the samples bonded at 160 °C for 30 min with or without the formic acid vapor were further inspected by cross-section observation, as shown in Figure 7. Agreeing well with the results of shear strength and fracture observation, the sintered structure of the sample bonded with the formic acid vapor is indeed much denser than that without the formic acid vapor, which further demonstrates that the formic acid vapor is beneficial for the sintering of Ag_2O microparticles. In the sintered layer of the sample without the formic acid vapor, there are still lots of visible nanoparticles, which indicates a poor sintering. Although this sintered layer seems much more loose than that in Figure 4a, we consider them to be consistent. In the case of sintering-bonding under pressure, where there should have been a slower out-diffusion of the oxygen-containing gas, the oxygen content at the interfacial layer became much higher, leading to a poor sintering with a loose structure.

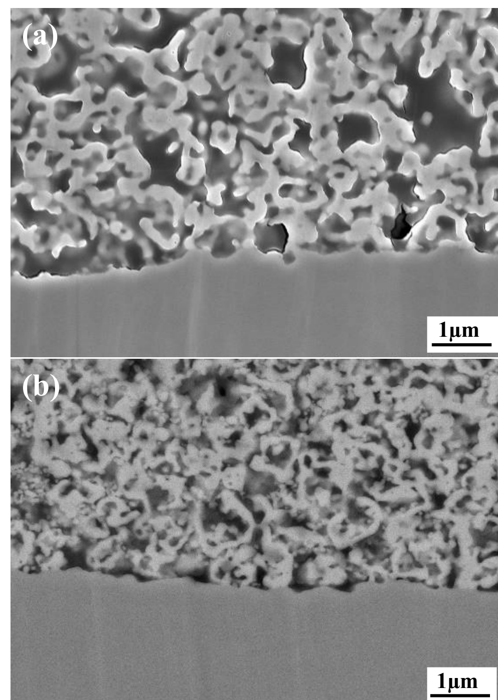

Figure 7. Cross-sectional SEM images of the interfacial microstructure of the sample bonded at 160 °C for 30 min (**a**) with and (**b**) without formic acid vapor.

Figure 8 shows the TEM images of a local interface between the sintered Ag and the Cu substrate with and without the formic acid treatment. As shown in Figure 8a, the bonding with the formic acid vapor achieved an interface of Ag-Cu without an interfacial oxide layer. Figure 8b,c are the fast Fourier transform (FFT) images corresponding to the two square areas in Figure 8a. At this location, the $(2\bar{2}0)$ lattice of the Ag is approximately parallel to the (111) lattice of the Cu. Besides, the interface has an approximately 5 nm-wide intermediate distorted layer with many dislocations (mainly in the Ag side). The origin of this interfacial distortion is considered to be the lattice mismatch between Ag and Cu (Ag: 4.086 Å versus Cu: 3.615 Å). One may also doubt whether the distorted layer is caused by the interdiffusion between Ag and Cu. The diffusion length d can be simply evaluated by $d = \sqrt{2Dt}$ [38]. Here, $\boldsymbol{D}$ is the diffusion coefficient, which is given by the Arrhenius equation $D = D_0 \exp(-Q/RT)$, D_0 is an oscillator factor, Q is the activation energy of diffusion, R is the gas constant, and T is the temperature in Kelvin. The activation energy of diffusion for Ag into Cu is 46.6 kcal mol^{-1}, whereas that of Cu in Ag is 46.1 kcal mol^{-1}; ${D_0}^{Ag\rightarrow Cu}$ was 0.61 cm^2 s^{-1}, and ${D_0}^{Cu\rightarrow Ag}$ was 1.23 cm^2 s^{-1} [39]. At 160 °C, $D^{Ag\rightarrow Cu}$ was 1.93×10^{-24} cm^2 s^{-1} and $D^{Cu\rightarrow Ag}$ was 6.97×10^{-24} cm^2 s^{-1}. The diffusion lengths of Ag in Cu and Cu in Ag were estimated to be 8.34×10^{-4} and 1.58×10^{-3} nm, respectively, which are neglectable. Thus, an Ag-Cu metallic bond contact without an interfacial solid solution and

an intermetallic compound at the interface can be confirmed, which is in conjunction with the lattice structure and Ag-Cu phase diagram [40]. For the bonding without the formic acid treatment, CuO formed adjacent to the sintered Ag, as shown in Figure 8d, which demonstrates the serious oxidation of the Cu surface. Figure 8e,f are the FFT images corresponding to the two square areas in Figure 8d. The distance of the (020) lattice of sintered Ag adjacent to the bonding interface has a variation and is not exactly the same as the typical values, which may be due to the unperfect crystallization at a restricted environment (CuO heterosurface and high oxygen concentration).

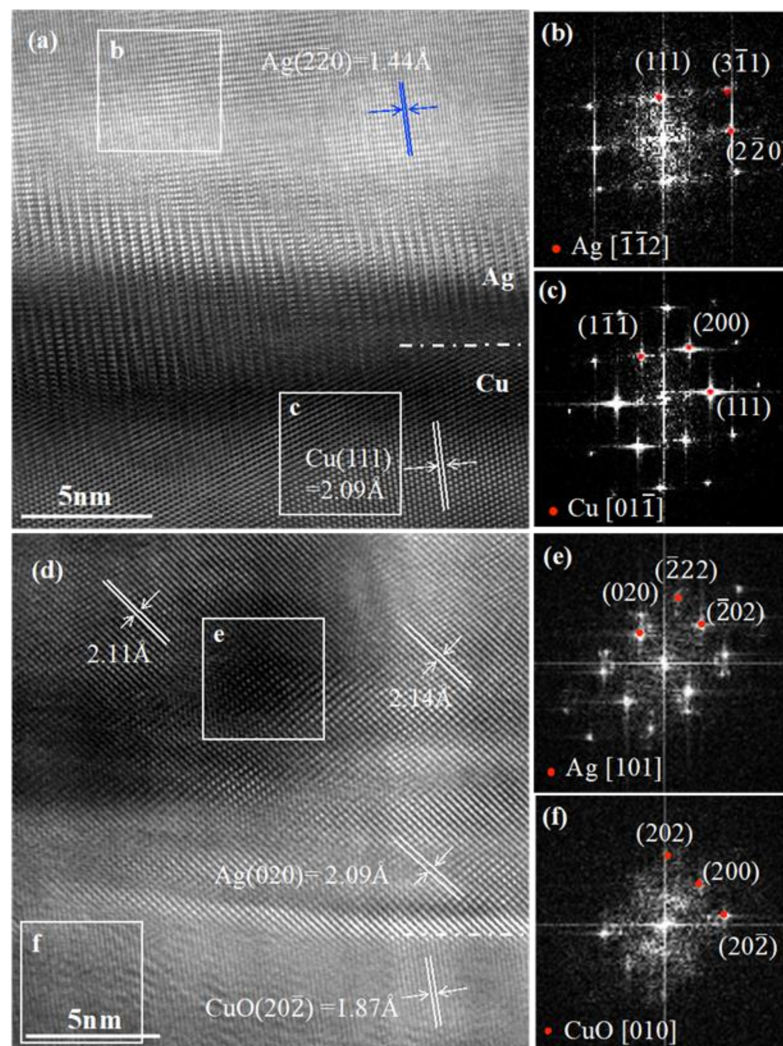

Figure 8. Scanning transmission electron microscope (STEM) image of a local interface between the sintered Ag and the Cu substrate: (**a**) with and (**d**) without formic acid treatment. (**b**,**c**) are the fast Fourier transform (FFT) images corresponding to the squared areas in (**a**), and (**e**,**f**) are the FFT images corresponding to the squared areas in (**d**). The bonding time is 30 min.

Figure 9 illustrates the analysis results of XPS. As shown in Figure 9a,b, respectively, the deconvoluted spectra of Cu $2P_{3/2}$ and Cu LMM further confirmed that the formation of CuO on the Cu substrate was caused by the decomposition of Ag_2O under N_2 environment. On the contrary, no CuO was generated with the Pt-catalyzed formic acid, which further demonstrated the reduction ability of the Pt-catalyzed formic acid vapor. The appearance of the $Cu_2O/Cu(OH)_2$ peak is caused by the surface exposure to air during sample preparation.

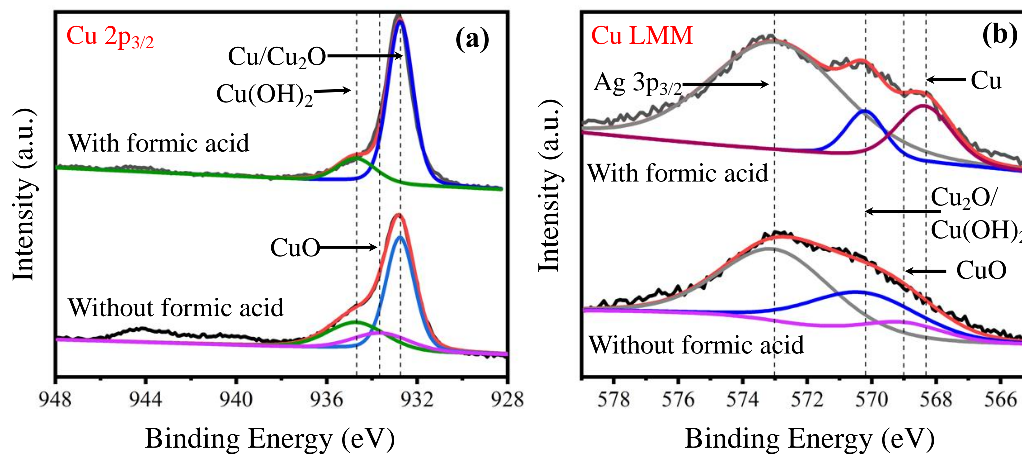

Figure 9. XPS spectra of the Cu surfaces after removal of the sintered Ag layer: (**a**) $Cu2p_{3/2}$ and (**b**) Cu LMM.

4. Conclusions

In summary, we achieved a strong sintering bonding of Ag-Cu at an ultra-low temperature of 160 °C under 3 MPa via the Ag nanoparticles in situ derived from Ag_2O microparticles with the assistance of the Pt-catalyzed formic acid vapor. The bonding for 10 min can achieve an average shear strength of approximately 22.8 MPa and it achieves an interface of a metallic bond of Ag-Cu free of Cu oxide layer, solid-solution, and intermetallic phases. By comparison with the bonding without the Pt-catalyzed formic acid vapor, the reduction ability of the Pt-catalyzed formic acid vapor is proved to be helpful for the sintering of Ag_2O microparticles and the removal of the interfacial Cu oxide layer between the sintered Ag and the Cu substrate. This ultra-low temperature Ag-Cu bonding sheds light on new opportunities for the structure design and material selection in power device packaging.

Author Contributions: Conceptualization, F.M. and X.W.; methodology, F.M., Y.W., and T.S.; investigation, L.H. and J.L.; writing—original draft preparation, F.M., X.W., and L.H.; writing—review and editing, F.M., X.W., and Y.W.; supervision, F.M., Y.W., and T.S.; project administration, Y.L., Y.W., and T.S.; funding acquisition, Y.W. and T.S. All authors have read and agreed to the published version of the manuscript.

Funding: This work was supported by the "100 Talents Project" of Chinese Academy of Sciences (Grant No.Y6YB02F001).

Conflicts of Interest: The authors declare no conflict of interest.

References

1. Lu, G.Q.; Calata, J.N.; Zhang, Z.; Bai, J.G. A lead-free, low-temperature sintering die-attach technique for high-performance and high-temperature packaging. In Proceedings of the 6th IEEE CPMT Conference on High Density Microsystem Design and Packaging and Component Failure Analysis (Hdp'04), Shanghai, China, 30 June–3 July 2004; pp. 42–46.
2. Zhang, H.Q.; Wang, W.G.; Bai, H.L.; Zou, G.S.; Liu, L.; Peng, P.; Guo, W. Microstructural and mechanical evolution of silver sintering die attach for SiC power devices during high temperature applications. *J. Alloys Compd.* **2019**, *774*, 487–494. [CrossRef]
3. Zhang, H.Q.; Bai, H.L.; Peng, P.; Guo, W.; Zou, G.S.; Liu, L. SiC chip attachment sintered by nanosilver paste and their shear strength evaluation. *Weld. World* **2019**, *63*, 1055–1063. [CrossRef]
4. Liu, X.D.; Nishikawa, H. Low-pressure Cu-Cu bonding using in-situ surface-modified microscale Cu particles for power device packaging. *Scr. Mater.* **2016**, *120*, 80–84. [CrossRef]
5. Manikam, V.R.; Cheong, K.Y. Die attach materials for high temperature applications: A review. *IEEE Trans. Compon. Packag. Manuf. Technol.* **2011**, *1*, 457–478. [CrossRef]
6. Zhao, Z.Y.; Zhang, H.Q.; Zou, G.S.; Ren, H.; Zhuang, W.D.; Liu, L.; Zhou, Y.N. A predictive model for thermal conductivity of nano-Ag sintered interconnect for a SiC die. *J. Electron. Mater.* **2019**, *48*, 2811–2825. [CrossRef]

7. Zhao, Z.; Zou, G.; Zhang, H.; Ren, H.; Liu, L.; Norman Zhou, Y. The mechanism of pore segregation in the sintered nano Ag for high temperature power electronics applications. *Mater. Lett.* **2018**, *228*, 168–171. [CrossRef]
8. Jiu, J.T.; Zhang, H.; Nagao, S.; Sugahara, T.; Kagami, N.; Suzuki, Y.; Akai, Y.; Suganuma, K. Die-attaching silver paste based on a novel solvent for high-power semiconductor devices. *J. Mater. Sci.* **2016**, *51*, 3422–3430. [CrossRef]
9. Jiu, J.T.; Zhang, H.; Koga, S.; Nagao, S.; Izumi, Y.; Suganuma, K. Simultaneous synthesis of nano and micro-Ag particles and their application as a die-attachment material. *J. Mater. Sci. Mater. Electron.* **2015**, *26*, 7183–7191. [CrossRef]
10. Guo, W.; Zhang, H.Q.; Zhang, X.Y.; Liu, L.; Peng, P.; Zou, G.S.; Zhou, Y.N. Preparation of nanoparticle and nanowire mixed pastes and their low temperature sintering. *J. Alloys Compd.* **2017**, *690*, 86–94. [CrossRef]
11. Feng, B.; Shen, D.; Wang, W.; Deng, Z.; Lin, L.; Ren, H.; Wu, A.; Zou, G.; Liu, L.; Zhou, Y.N. Cooperative bilayer of lattice-disordered nanoparticles as room-temperature sinterable nanoarchitecture for Device Integrations. *ACS Appl. Mater. Interface* **2019**, *11*, 16972–16980. [CrossRef]
12. Nishikawa, H.; Liu, X.D.; Wang, X.F.; Fujita, A.; Kamada, N.; Saito, M. Microscale Ag particle paste for sintered joints in high-power devices. *Mater. Lett.* **2015**, *161*, 231–233. [CrossRef]
13. Hirose, A.; Tatsumi, H.; Takeda, N.; Akada, Y.; Ogura, T.; Ide, E.; Morita, T. A novel metal-to-metal bonding process through in-situ formation of Ag nanoparticles using Ag_2O microparticles. *J. Phys. Conf. Ser.* **2009**, *165*, 012074. [CrossRef]
14. Gao, Y.; Zhang, H.; Li, W.L.; Jiu, J.T.; Nagao, S.; Sugahara, T.; Suganuma, K. Die bonding performance using bimodal Cu particle paste under different sintering atmospheres. *J. Electron. Mater.* **2017**, *46*, 4575–4581. [CrossRef]
15. Kobayashi, Y. Preparation of copper nanoparticles and metal-metal bonding process using them. *World J. Eng.* **2013**, *10*, 113–118. [CrossRef]
16. Ren, H.; Mu, F.W.; Shin, S.; Liu, L.; Zou, G.S.; Suga, T. Low temperature Cu bonding with large tolerance of surface oxidation. *AIP Adv.* **2019**, *9*, 055127. [CrossRef]
17. Wu, C.J.; Chen, S.M.; Sheng, Y.J.; Tsao, H.K. Anti-oxidative copper nanoparticles and their conductive assembly sintered at room temperature. *J. Taiwan Inst. Chem. Eng.* **2014**, *45*, 2719–2724. [CrossRef]
18. Zhao, J.; Yao, M.; Lee, N. Nano-Cu sintering paste for high power devices die attach applications. In Proceedings of the 2018 IEEE 68th Electronic Components and Technology Conference (ECTC), San Diego, CA, USA, 29 May–1 June 2018; pp. 557–563.
19. Morita, T.; Yasuda, Y.; Ide, E.; Akada, Y.; Hirose, A. Bonding technique using micro-scaled silver-oxide particles for in-situ formation of silver nanoparticles. *Mater. Trans.* **2008**, *49*, 2875–2880. [CrossRef]
20. Mu, F.W.; Zhao, Z.Y.; Zou, G.S.; Bai, H.L.; Wu, A.P.; Liu, L.; Zhang, D.Y.; Norman Zhou, Y. Mechanism of low temperature sintering-bonding through in-situ formation of silver nanoparticles using silver oxide microparticles. *Mater. Trans.* **2013**, *54*, 872–878. [CrossRef]
21. Chen, C.; Luo, F.; Kang, Y. A review of SiC power module packaging: Layout, material system and integration. *CPSS Trans. Power Electron. Appl.* **2017**, *2*, 170–186. [CrossRef]
22. Zhang, Z.; Chen, C.T.; Yang, Y.; Zhang, H.; Kim, D.; Sugahara, T.; Nagao, S.; Suganuma, K. Low-temperature and pressureless sinter joining of Cu with micron/submicron Ag particle paste in air. *J. Alloys Compd.* **2019**, *780*, 435–442. [CrossRef]
23. Zheng, H.; Berry, D.; Ngo, K.D.T.; Lu, G. Chip-bonding on copper by pressureless sintering of nanosilver paste under controlled atmosphere. *IEEE Trans. Compon. Packag. Manuf. Technol.* **2014**, *4*, 377–384. [CrossRef]
24. Zhao, S.Y.; Li, X.; Mei, Y.H.; Lu, G.Q. Novel interface material used in high power electronic die-attaching on bare Cu substrates. *J. Mater. Sci. Mater. Electron.* **2016**, *27*, 10941–10950. [CrossRef]
25. Chen, C.T.; Zhang, Z.; Kim, D.; Zhang, B.; Tanioku, M.; Ono, T.; Matsumoto, K.; Suganuma, K. Interfacial oxidation protection and thermal-stable sinter Ag joining on bare Cu substrate by single-layer graphene coating. *Appl. Surf. Sci.* **2019**, *497*, 143797. [CrossRef]
26. Takata, S.; Ogura, T.; Ide, E.; Morita, T.; Hirose, A. Effects of solvents in the polyethylene glycol serieson the bonding of copper joints using Ag_2O paste. *J. Electron. Mater.* **2013**, *42*, 507–515. [CrossRef]
27. Suzuki, Y.; Ogura, T.; Takahashi, M.; Hirose, A. Low-current resistance spot welding of pure copper using silver oxide paste. *Mater. Charact.* **2014**, *98*, 186–192. [CrossRef]

28. Ogura, T.; Takata, S.; Takahashi, M.; Hirose, A. Effects of reducing solvent on copper, nickel, and aluminum joining using silver nanoparticles derived from a silver oxide paste. *Mater. Trans.* **2015**, *56*, 1030–1036. [CrossRef]
29. Yang, W.; Shintani, H.; Akaike, M.; Suga, T. Low temperature Cu-Cu direct bonding using formic acid vapor pretreatment. In Proceedings of the 2011 IEEE 61st Electronic Components and Technology Conference (ECTC), Lake Buena Vista, FL, USA, 31 May–3 June 2011; pp. 2079–2083.
30. Yang, W.H.; Akaike, M.; Fujino, M.; Suga, T. A combined process of formic acid pretreatment for low-temperature bonding of copper electrodes. *ECS J. Solid State Sci. Technol.* **2013**, *2*, 271–274. [CrossRef]
31. Yang, W.; Akaike, M.; Fujino, M.; Suga, T. Formic acid with Pt catalyst combined treatment process for Cu low temperature bonding. In Proceedings of the 2012 13th International Conference on Electronic Packaging Technology and High Density Packaging (ICEPT), Guilin, China, 13–16 August 2012; pp. 147–150.
32. Yang, W.; Akaike, M.; Suga, T. Effect of formic acid vapor in situ treatment process on Cu low-temperature bonding. *IEEE Trans. Compon. Packag. Manuf. Technol.* **2014**, *4*, 951–956. [CrossRef]
33. Yang, W.; Shintani, H.; Akaike, M.; Suga, T. Formic acid vapor treated Cu-Cu direct bonding at low temperature. In Proceedings of the 2011 12th International Conference on Electronic Packaging Technology and High Density Packaging (ICEPT), Shanghai, China, 8–11 August 2011; pp. 1–4.
34. Yang, W.; Lu, Y.; Tadatomo, S. The study of Cu-Cu low temperature bonding using formic acid treatment with/without Pt catalyst. In Proceedings of the 2016 17th International Conference on Electronic Packaging Technology (ICEPT), Wuhan, China, 16–19 August 2016; pp. 784–787.
35. Suga, T.; Masakate, A.; Wenhua, Y.; Matsuoka, N. Formic acid treatment with Pt catalyst for Cu direct bonding at low temperature. In Proceedings of the 2014 International Conference on Electronics Packaging (ICEP), Toyama, Japan, 23–25 April 2014; pp. 644–647.
36. Fujino, M.; Akaike, M.; Matsuoka, N.; Suga, T. Reduction reaction analysis of nanoparticle copper oxide for copper direct bonding using formic acid. *Jpn. J. Appl. Phys.* **2017**, *56*, 04CC01. [CrossRef]
37. Lee, S.K.; Hsu, H.C.; Tuan, W.H. Oxidation behavior of copper at a temperature below 300 degrees C and the methodology for passivation. *Mater. Res.* **2016**, *19*, 51–56. [CrossRef]
38. Bokstein, B.S.; Mendelev, M.I.; Srolovitz, D.J. *Thermodynamics and Kinetics in Materials Science a Short Course*, 1st ed.; Oxford University Press: Oxford, UK, 2005; pp. 165–188.
39. Butrymowicz, D.B.; Manning, J.R.; Read, M.E. Diffusion in copper and copper alloys, part II. copper-silver and copper-gold systems. *J. Phys. Chem. Ref. Data* **1974**, *3*, 527–602. [CrossRef]
40. Fukikoshi, T.; Watanabe, Y.; Miyazawa, Y.; Kanasaki, F. Brazing of copper to stainless steel with a low-silver-content brazing filler metal. *IOP Conf. Ser. Mater. Sci. Eng.* **2014**, *61*, 012016. [CrossRef]

© 2020 by the authors. Licensee MDPI, Basel, Switzerland. This article is an open access article distributed under the terms and conditions of the Creative Commons Attribution (CC BY) license (http://creativecommons.org/licenses/by/4.0/).